

Binary Mixtures of Bose Condensates of Alkali Atoms

Tin-Lun Ho and V. B. Shenoy

Physics Department, The Ohio State University, Columbus, Ohio 43210

(Received 20 May 1996)

We show that binary mixtures of Bose condensates of alkali atoms have a great variety of ground state and vortex structures which can be accessed experimentally by varying the particle numbers of different alkalis. We have constructed a simple algorithm to determine the density profiles of the mixtures within Thomas-Fermi approximation. Many structures of the alkali binary contain a coexisting region, which is the analog of the long sought ^3He - ^4He interpenetrating superfluids in ultralow temperature physics. [S0031-9007(96)01390-7]

PACS numbers: 03.75.Fi, 05.30.Jp

The search of Bose condensate in alkali atoms [1–3] has a deep root in ultralow temperature physics. Since the discovery of superfluid ^3He , the searches of the next elemental superfluid have been focusing on spin polarized hydrogen and ^3He - ^4He mixture. The former promises another Bose superfluid besides the only known example of ^4He , the latter, the first example of interpenetrating superfluids. The recent discoveries of alkali Bose condensates [1–3] have in essence achieved the goal of the superfluid hydrogen search. Since there are no intrinsic difficulties in loading more than one alkali element and having them cooled in the same trap, it appears highly promising that interpenetrating superfluids may be realized for the first time within the same experimental setting.

In this paper, we shall discuss binary mixtures of alkali condensates. Such mixtures may consist of different alkalis such as ^{87}Rb - ^{23}Na , or different isotopes such as ^{87}Rb - ^{85}Rb , or different hyperfine states of the same alkali such as the ($F = 2, M_F = 2$) and ($F = 1, M_F = 1$) states of ^{87}Rb . We shall denote the two different alkalis as 1 and 2, and their particle numbers as N_1 and N_2 . Unlike single component systems which are characterized by a single scattering length, alkali binaries are characterized by three scattering lengths a_1, a_2 , and a_{12} , representing interactions between like and unlike alkalis. At present, the scattering lengths between many like alkali atoms are known, whereas those between unlike alkalis have not been measured. As we shall see, this moderate increase in energy scales leads to a proliferation of ground state and vortex structures.

In the following, we shall present (a) a simple algorithm for determining the density profiles of the mixtures, (b) the evolution of the ground states and vortex states as a function of N_1, N_2 . For length reasons, we shall limit ourselves to the vortex states where alkali 1 contains a 2π vortex and alkali 2 is vortex free. Our algorithm, however, can be applied to an arbitrary number of vortices in 1 and 2. As we shall see, the structure of the mixture depends on the ratio of g factors of the two alkalis and the ratios of their interaction parameters. These ratios determine whether alkali 2 when added to an existing cloud of 1 will stay at its exterior or interior. Another general feature of

the mixture is that when $N_1 \sim N_2$, it generally contains a large coexisting region of 1 and 2. This is the analog of the long sought ^3He - ^4He superfluid mixture in ultralow temperature physics.

Our results are obtained by minimizing the Gross-Pitaevskii energy $E(\Psi_1, \Psi_2)$ subject to the constraint of constant particle numbers, i.e., by the condition $\delta K = 0$, $K \equiv E(\Psi_1, \Psi_2) - \mu_1 N_1 - \mu_2 N_2$, where (Ψ_i, μ_i) are the order parameter and chemical potential of the i th alkali, $i = 1, 2$. The energy is of the form $E = T + U + V$, where T , U , and V are the kinetic energy, the potential energy of the magnetic trap, and the interaction energy between alkali atoms. The kinetic energy is $T = \int (\sum_{i=1,2} (\hbar^2/2M_i) |\nabla\Psi_i|^2 + \zeta_1 \Psi_1^* \nabla\Psi_1 \Psi_2^* \nabla\Psi_2 + \zeta_2 \Psi_1^* \nabla\Psi_1 \Psi_2 \nabla\Psi_2^* + \text{c.c.})$, where ζ_1 and ζ_2 are complex coefficients caused by backflow effects between different alkalis. They are expected to be small in the dilute limit. The trap potentials $U = \sum_{i=1,2} U_i(\mathbf{x}) |\Psi_i|^2$ are of the form [4]

$$U_i(\mathbf{x}) = \frac{g_i \mu_B B_0}{2L^2} (r^2 + \lambda^2 z^2) \equiv \frac{1}{2} M_i \omega_i^2 (r^2 + \lambda^2 z^2),$$

$M_1 \omega_1^2 / (M_2 \omega_2^2) = g_1 / g_2$ where λ is the trap anisotropy, g_i and M_i are the g factor and mass of the i th alkali, μ_B is the Bohr magneton, B_0 is the magnetic field at the center of the trap, and L is the length scale of the variations of the magnetic field. For dilute Bose gases, since the scattering between both like and unlike alkali are dominated by s -wave scattering, we have

$$V = \frac{1}{2} \int d\mathbf{x} (G_1 |\Psi_1|^4 + G_2 |\Psi_2|^4 + 2G_{12} |\Psi_1|^2 |\Psi_2|^2),$$

where $G_i = 4\pi \hbar^2 a_i / M_i$, $i = 1, 2$; $G_{12} = 2\pi \hbar^2 a_{12} / \sqrt{M_1 M_2}$.

For large N_1, N_2 , the minimization can be done with great accuracy in the Thomas-Fermi approximation (TFA) [5], which ignores all $\nabla|\Psi_i|$ terms in T . For vortex free structures [denoted as (v0)], this amounts to setting $T = 0$. If alkali 1 has a 2π vortex while alkali 2 is vortex free [denoted as (v1)] (i.e., $\Psi_1 = |\Psi_1| e^{i\phi}$ and $\Psi_2 = |\Psi_2|$), TFA amounts to retaining only the centrifugal term

$|\Psi_1|^2/r^2$ in T . By rescaling $z \rightarrow z/\lambda$, the functional K within TFA takes the simple form

$$K = \int [-\tilde{\mu}_1 \rho_1 - \tilde{\mu}_2 \rho_2 + \frac{1}{2}(G_1 \rho_1^2 + G_2 \rho_2^2 + 2G_{12} \rho_1 \rho_2)],$$

$$\rho_i \equiv |\Psi_i|^2,$$

$$\begin{aligned} \tilde{\mu}_1 &= \mu_1(z) - \frac{M_1 \omega_1^2 r^2}{2} - \frac{\hbar^2}{2M_1} \frac{p}{r^2}, \\ \tilde{\mu}_2 &= \mu_2(z) - \frac{M_2 \omega_2^2 r^2}{2}, \end{aligned} \quad (1)$$

where $p = 0$ and 1 for (v0) and (v1) states, respectively, and $\mu_i(z)$ are defined as $\mu_i(z) \equiv \mu_i - \frac{1}{2} M_i \omega_i^2 z^2, i = 1, 2$.

Our goal is to find the density profile (ρ_1, ρ_2) as a function of particle number $N_1, N_2, (N_i = \int \rho_i)$. This is done by the following: (I) Minimizing K to find the equilibrium densities ρ_i for given chemical potential μ_i . (II) Use the relation $(N_i = \int \rho_i)$ to obtain N_i as a function of μ_i [i.e., $N_i = N_i(\mu_1, \mu_2)$]. (III) Inverting the relation to obtain $\mu_i = \mu_i(N_1, N_2)$, which immediately gives ρ_i as

a function of (N_1, N_2) because of (I). Although much of our labor went into (II) and (III), they are straightforward (though lengthy) calculations once the densities profiles are determined by the simpler but subtler step (I), which we now discuss.

Constructing ρ_1, ρ_2 for given μ_1, μ_2 .—Let [0], [1], [2], [12] denote the vacuum, the single phase of 1, 2, and the coexisting phase of 1 and 2, respectively. The densities of these phases are given by the stationary conditions of K . The vacuum [0] is given by $\rho_1 = \rho_2 = 0$. The stationary conditions of the other three phases are (with $\rho_i \geq 0$) [12] $\rho_1 = (G_2 \tilde{\mu}_1 - G_{12} \tilde{\mu}_2)/(G_1 G_2 - G_{12}^2), \rho_2 = (G_1 \tilde{\mu}_2 - G_{12} \tilde{\mu}_1)/(G_1 G_2 - G_{12}^2)$; [1] $\rho_1 = \tilde{\mu}_1/G_1, \rho_2 = 0$; and [2] $\rho_2 = \tilde{\mu}_2/G_2, \rho_1 = 0$. The distribution of these “phases” in the $\tilde{\mu}_1$ - $\tilde{\mu}_2$ plane will be referred to the *distribution plot*. A distribution plot for positive G_{12} is shown in Figs. 1.1 and 1.2. The boundaries (or interfaces) separating [12] from [2] and [1] are denoted as $\mathbf{1}_0$ and $\mathbf{2}_0$. They are the surfaces of vanishing ρ_1 and ρ_2 , described by

$$\mathbf{1}_0 : \tilde{\mu}_2 = [G_2/G_{12}] \tilde{\mu}_1, \quad \mathbf{2}_0 : \tilde{\mu}_2 = [G_{12}/G_1] \tilde{\mu}_1. \quad (2)$$

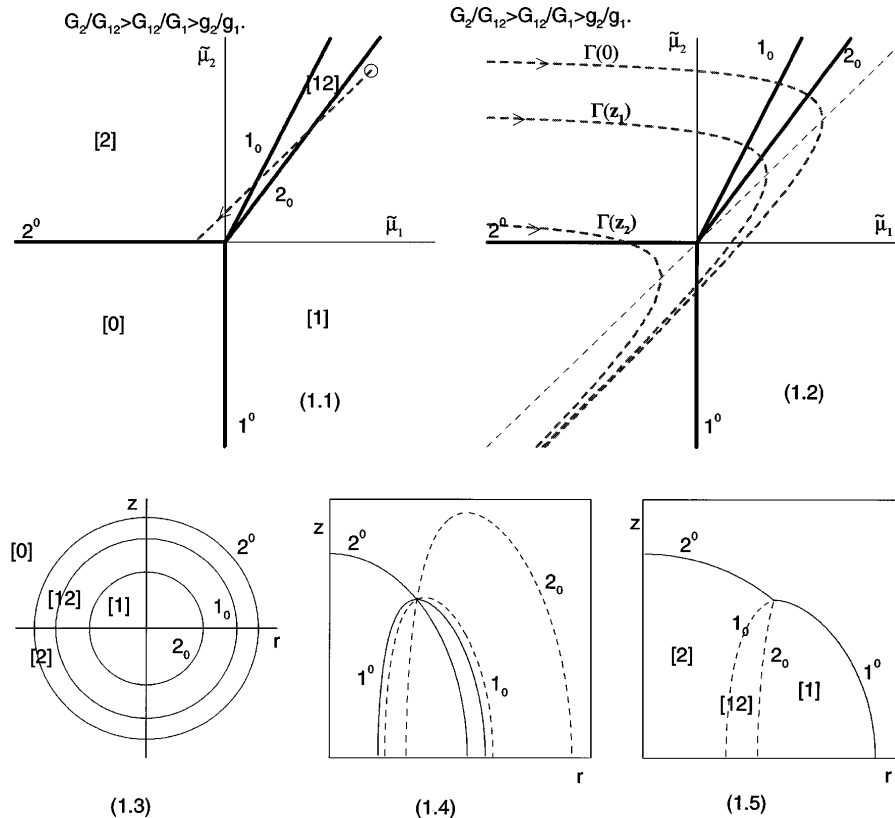


FIG. 1. 1.1 and 1.2 show the typical distribution plots for $G_{12} > 0, G_2/G_{12} > G_{12}/G_1 > 1$. The “image paths” $\Gamma(z)$ (dashed lines) of the ground state (v0) and the (v1) vortex are shown as dashed lines in these figures. The circle in 1.1 denotes the point $[\mu_1(z), \mu_2(z)]$. The slope of the dotted line is g_2/g_1 . In 1.2, the image path $\Gamma(z)$ is shown for different values of $z (z_2 > z_1 > 0)$. As z increases, $\Gamma(z)$ slides down rigidly along the straight line with slope g_2/g_1 . 1.3 shows the interfaces $(\mathbf{2}_0, \mathbf{1}_0, \mathbf{2}^0)$ in 1.1 intersected by $\{\Gamma(z)\}$. They are spherical surfaces as given by Eqs. (2) and (1) with $p = 0$. 1.4 shows that boundary surfaces $(\mathbf{1}_0, \mathbf{2}_0, \mathbf{1}^0, \mathbf{2}^0)$ cut by $\{\Gamma(z)\}$ in 1.2. They are given by Eqs. (2) and (1) with $p = 1$. Only one quadrant of the interface structure is shown as it is cylindrical symmetric. Eliminating the portion of surfaces in 1.4 inconsistent with the order of intersections shown in 1.2, we are left with the interfaces in 1.5, which is the structure of the (v1) vortex.

The interfaces separating the vacuum $[0]$ from $[1]$ and $[2]$ are denoted as 1^0 and 2^0 . They are described by equations ($1^0 : \tilde{\mu}_1 = 0$) and ($2^0 : \tilde{\mu}_2 = 0$).

From Eq. (1), we note that a path in real space will induce an "image" in $\tilde{\mu}_1$ - $\tilde{\mu}_2$ space. For example, a radial path on the horizontal plane with height z will induce an image $\Gamma(z)$ in $\tilde{\mu}_1$ - $\tilde{\mu}_2$ plane as $\Gamma(z)$:

$$[\tilde{\mu}_1 - \mu_1(z)](\hbar\omega_1/2) = [g_1/g_2][\tilde{\mu}_2 - \mu_2(z)]/(\hbar\omega_1/2) + p\{(g_1/g_2)[\tilde{\mu}_2 - \mu_2(z)] \times (\hbar\omega_1/2)\}^{-1}.$$

For vortex free states ($p = 0$), $\Gamma(z)$ is a straight line with slope g_2/g_1 emerging from the point $(\mu_1(z), \mu_2(z))$, which is shown as a dashed line and a circle in Fig. 1.1. For (v1) vortices, $\{\Gamma(z)\}$ is a family of curves shown in Fig. 1.2, with $z_2 > z_1 > 0$. The arrows on these paths indicate the direction of increasing r . As r varies from 0 to ∞ , $\Gamma(z)$ intersects the phase boundaries in a specific order. From the definition of $\mu_i(z)$, it is easy to see that as $|z|$ increases, $\Gamma(z)$ slides down rigidly along the straight line with slope g_2/g_1 .

The above considerations suggest a simple algorithm for determining the structure of the mixture: (i) For given chemical potentials μ_1, μ_2 , draw the image paths $\{\Gamma(z)\}$ on the distribution plot. $\Gamma(z)$ will intersect a set of phase boundaries in a specific order. (ii) Using Eqs. (2) and (1), construct in real space the set of boundary surfaces (i.e.,

$\{1_0, 2_0, 1^0, 2^0\}$) intersected by $\{\Gamma(z)\}$. (iii) Eliminate all portions of these boundary surfaces that are inconsistent with the order of intersections generated in (i). The remaining surfaces are the physical boundaries in the mixture.

To illustrate this algorithm, consider the vortex free mixture in Fig. 1.1. The image paths of this mixture intersect phase boundaries $2_0, 1_0$, and 2^0 . From Eqs. (2) and (1), it is easily seen that these boundary curves (or interfaces) are spherical surfaces separating the single component and coexisting regions as shown in Fig. 1.3. Figure 1.3 is the structure of the mixture. For the (v1) vortex in Fig. 1.2, the family $\{\Gamma(z)\}$ intersects all four phase boundaries ($1_0, 2_0, 1^0, 2^0$) in the order ($1_0 2_0 1^0$, or 2^0 alone). Displaying all four boundary surfaces using Eqs. (2) and (1) (see Fig. 1.4) and eliminating all sections of these surfaces inconsistent with the order of intersection, we obtain the physical boundaries shown in Fig. 1.5.

Determination of density profile as a function of particle numbers N_1, N_2 .—Having determined the density profiles for given chemical potential (μ_1, μ_2), we have followed steps (II) and (III) mentioned above to construct the phase diagrams for both ground states (v0) and vortex states (v1) over the entire range of (G_1, G_2, G_{12} , and g_1/g_2). In general, the phase diagram depends on the interaction ratios $G_1/G_{12}, G_{12}/G_2$, and the g -factor ratios g_2/g_1 . The entire phase diagram is too rich to be displayed in the limited space here. Instead, we shall show the evolution of the density profile as a function of

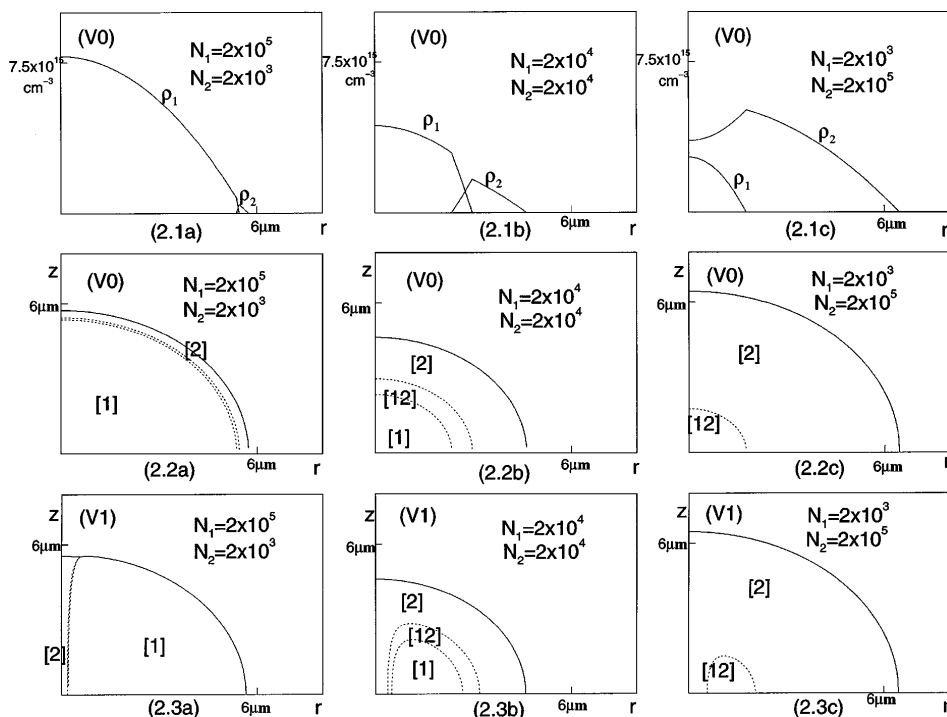


FIG. 2. Case (a): $(G_1, G_2, G_{12}) = (9.604, 17.78, 12.52) \times 10^{-38}$ ergs cm^3 . 2.1(a) to 2.1(c) show the ground state structure of the mixture for different N_1, N_2 for the case $G_2/G_{12} > G_{12}/G_1 > 1$. The interfaces of these structures are shown in 2.2(a) to 2.2(c). When a 2π vortex is inserted into alkali 1, these interfaces change to those in 2.3(a) to 2.3(c). The narrow region between the two dotted lines in 2.2(a) is the coexistence region $[12]$.

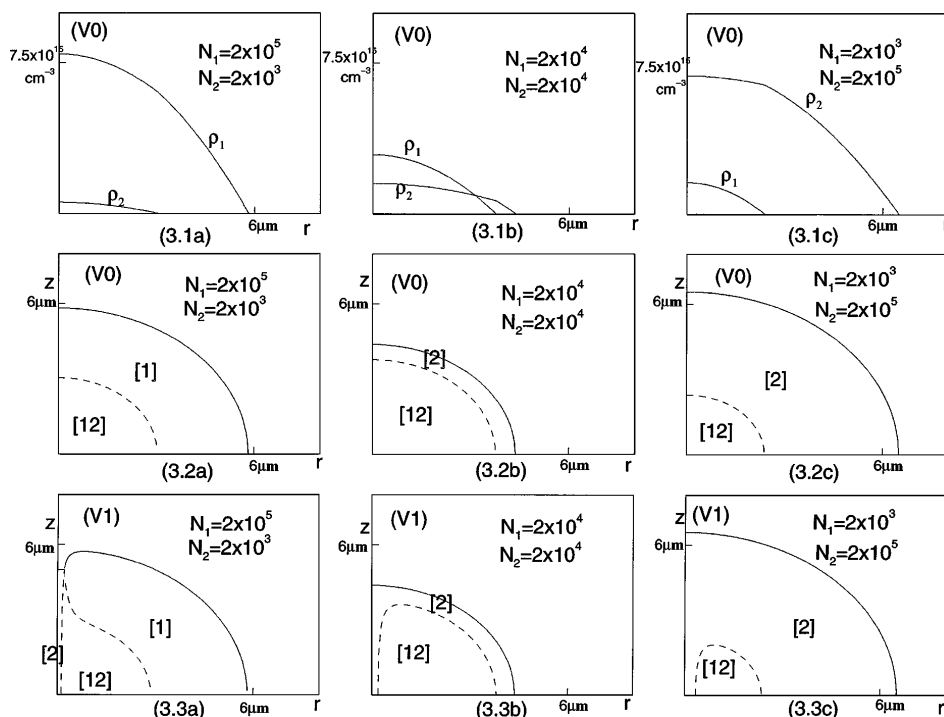


FIG. 3. Case (b): $(G_1, G_2, G_{12}) = (9.604, 17.78, 6.636) \times 10^{-38}$ ergs cm^3 . 3.2(a) to 3.2(c) show the ground state structure of the mixture for different N_1, N_2 for the case $G_2/G_{12} > 1 > G_{12}/G_1$. The interfaces of these structures are shown in 3.2(a) to 3.2(c). The interfaces of the (v1) vortices with the same N_1, N_2 are shown in 3.3(a) to 3.3(c).

N_1, N_2 for the cases (a) $G_2/G_{12} > G_{12}/G_1 > g_2/g_1$ and (b) $G_2/G_{12} > g_2/g_1 > G_{12}/G_1$.

We shall use the ^{87}Rb - ^{23}Na mixture as an example, with Rb and Na denoted as 1 and 2, respectively. We then have $g_2/g_1 = 1$, $G_1 = 9.604 \times 10^{-38}$ erg cm^3 , $G_2 = 17.871 \times 10^{-38}$ erg cm^3 [6]. The two cases (a) and (b) we considered are $G_{12} = 12.52 \times 10^{-38}$ erg cm^3 and $G_{12} = 6.636 \times 10^{-38}$ erg cm^3 , respectively. The trap is taken to be isotropic ($\lambda = 1$). In going through steps (II) and (III), one also needs the trap frequencies $\omega_i = 2\pi f_i$. Taking $f_1 = 180$ Hz, and using the relation $\omega_1/\omega_2 = \sqrt{g_1 M_2/g_2 M_1}$, we have $f_2 = 350.1$ Hz.

The evolution of the density profiles of cases (a) and (b) as a function of N_1, N_2 are shown in Figs. 2 and 3. The ground states of these cases are shown in Figs. 2.1(a) to 2.1(c), and Figs. 3.1(a) to 3.1(c), respectively. Figure 2.1(a) shows that when atom 2 is added onto a large cloud of atom 1, it stays at the surface of the latter. On the other hand, Fig. 2.1(c) shows that when atom 1 is added onto a large cloud of 2, it enters into the interior of 2 directly. For case (b), Figs. 3.1(a) and 3.1(c) show that one species always enters into the center of the other. It is also useful to look at the structure of the mixtures in terms of the interfaces separating different phases. The interfaces of the ground states in Figs. 2.1(a) to 2.1(c) and those in Figs. 3.1(a) to 3.1(c) are shown in Figs. 2.2(a) to 2.2(c) and Figs. 3.2(a) to 3.2(c), respectively. When a 2π vortex is inserted in alkali 1 [i.e., the (v1) vortices], these interfaces become those in Figs. 2.3(a) to 2.3(c)

and Figs. 3.3(a) to 3.3(c). From the structures shown in Figs. 2 and 3, one sees that many of them contain a large region of coexisting phase [12].

Our discussions above show that by varying the particle numbers of the alkalis, one can go continuously from regimes of interpenetrating superfluids to those with separated phases. The possibility of scanning through this continuum offers great opportunities to study coupled macroscopic quantum phenomena of distinct Bose fluids, and widen our horizon on superfluid phenomenon.

T.L.H. would like to thank Greg Lafyatis and Nick Bigelow for discussions. This work is supported in part by NSF Grant No. DMR-9406936.

-
- [1] M.H. Anderson, J.R. Ensher, M.R. Mathews, C.E. Weiman, and E.A. Cornell, *Science* **269**, 198 (1995).
 - [2] C.C. Bradley, C.A. Sackett, J.J. Tollett, and R.G. Hulet, *Phys. Rev. Lett.* **75**, 1687 (1995).
 - [3] K.B. Davis, M.O. Mewes, M.R. Andrews, N.J. van Druten, D.S. Durfee, D.M. Kurn, and W. Ketterle, *Phys. Rev. Lett.* **75**, 3969 (1995).
 - [4] See T.L. Ho and V.B. Shenoy, *Phys. Rev. Lett.* **77**, 2595 (1996), for a derivation of this form of potentials in current magnetic traps.
 - [5] M. Edwards and K. Burnett, *Phys. Rev. A* **51**, 1382 (1995); G. Baym and C.J. Pethick, *Phys. Rev. Lett.* **76**, 6 (1996).
 - [6] The scattering lengths of ^{23}Na and ^{87}Rb are 49 and 100 Å, respectively.